ISSN 0027-1349, Moscow University Physics Bulletin, 2014, Vol. 69, No. 1, pp. 1–20. © Allerton Press, Inc., 2014.
Original Russian Text © B.S. Ishkhanov, M.E. Stepanov, T.Yu. Tretyakova, 2014, published in Vestnik Moskovskogo Universiteta. Fizika, 2014, No. 1, pp. 3–19.

Nucleon Pairing in Atomic Nuclei

B. S. Ishkhanov[a, b], M. E. Stepanov[a, b], and T. Yu. Tretyakova[b]

[a] *Department of Physics, Moscow State University, Moscow, 119991 Russia*

[b] *Skobel'tsyn Institute of Nuclear Physics, Moscow State University, Moscow, 119991 Russia*

e-mail: stepanov@depni.sinp.msu.ru, tretyakova@dubna.ru

Received September 10, 2013; in final form, November 6, 2013

Abstract—The nucleon pairing effect that is analyzed in the present paper is one of the striking manifestations of nuclear dynamics. Nucleon pairing for different chains of nuclei dependent upon the number of protons or neutrons in the nucleus allows one to explain the emergence of a great number of positive-parity states, which form a ground state multiplet, in even–even nuclei in the excitation energy range $E^* < 4$ MeV. The interaction of paired nucleons with vibrational and rotational degrees of freedom of a nucleus produces a wide variety of excitation spectra of positive-parity states in even–even nuclei.

Keywords: nucleon–nucleon interaction, models of atomic nuclei, nucleon pairing in atomic nuclei.

DOI: 10.3103/S0027134914010068

INTRODUCTION

One of the fundamental problems of nuclear physics lies in defining the properties of atomic nuclei based on nucleon–nucleon interaction. However, an atomic nucleus is such a complex system that several models that describe different aspects of nuclear dynamics necessarily emerge. Nucleon pairing is an important manifestation of the properties of atomic nuclei. In addition to a mean field formed by the interaction of all present nucleons, short-range nuclear attractive forces, which lead to nucleon pairing, act within an atomic nucleus. Such pairing of fermionic nucleons produces quasiparticles that are governed by Bose–Einstein statistics and this is manifested in the effect of superfluidity in atomic nuclei.

Atomic nuclei, which constitute 99.9% of the baryonic matter in the Universe are bound systems that are comprised of Z protons and N neutrons ($Z + N = A$, where A is the mass number of a nucleus).

The dependence of the central interaction of a pair of nucleons on the distance between them (r) is shown in Fig. 1. Nuclear forces are short-range: as nucleons are brought closer to each other, the attraction becomes stronger and is maximized at $r \approx 0.8$ fm, while at $r < 0.7$ fm this attraction turns into repulsion. The dependence shown in Fig. 1 takes only the central forces into account. The interaction between nucleons depends not only on the distance, but also on the spins of nucleons, their mutual alignment, and their orbital motion. Specifically, the only bound state of a pair of nucleons (a deuteron) corresponds to a dominant state with total angular momentum $J = 1$, orbital angular momentum $L = 0$, and codirectional spins of nucleons. The nucleon–nucleon interaction in atomic nuclei is complicated further by its dependence on neighboring nucleons: such an interaction in a vacuum differs from the interactions of nucleons in a nuclear medium.

The properties and structure of an atomic nucleus are highly dependent on the mass number (A) and on the ratio between the number of protons and the number of neutrons in the nucleus. Since the discovery of the atomic nucleus, considerable efforts have been exerted to construct a general theory of the nucleus that would cover the entire range of known nuclei and have strong predictive power. This problem becomes especially important in the present context, since modern experimental techniques and instruments allow one to gather data on exotic short-lived atomic nuclei and extend the isotope chart into the region of ultraheavy nuclei and nuclei with extreme ratios between the number of protons and the number of neutrons.

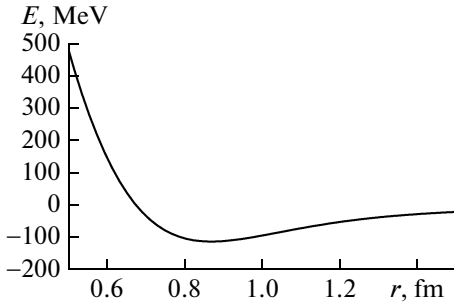

Fig. 1. *NN* interaction in the $^1S_0$ channel in the Argonne v_{18} potential [1].

The liquid-drop nuclear model is one of the fundamental models. Within the framework of this model, the nucleus is considered to be a charged liquid drop. This makes it possible to isolate the contributions of volume, surface, and Coulomb energies in the nuclear binding energy. This representation (with the inclusion of the symmetry energy) formed the basis of the semiempirical Bethe–Weizsácker formula [2, 3] for the mass of atomic nuclei:

$$M(N, Z) = Nm_n + Zm_p - E_{\text{bind}}(N, Z)/c^2,$$
$$E_{\text{bind}}(N, Z) = a_1 A - a_2 A^{2/3} - a_3 \frac{Z^2}{A^{1/3}} - \frac{1}{2} a_4 \frac{(N-Z)^2}{A}, \quad (1)$$

where $M(N, Z)$ is the mass of an atomic nucleus comprised of Z protons and N neutrons, E_{bind} is the nuclear binding energy (the minimum energy required to split a nucleus into its constituent nucleons), and m_n and m_p are the neutron and proton masses. Parameters a_1, a_2, a_3, and a_4 correspond to the contributions of the volume and surface energies, the Coulomb interaction, and the nuclear symmetry energy and are determined from the experimental data. The authors of [3] calculated the following values of the coefficients a_1, a_2, a_3, and a_4:

(i) The values of the coefficients $a_1 = 13.86$ MeV and $a_2 = 13.2$ MeV were chosen in such a way so as to reproduce the masses of ^{16}O and ^{200}Hg nuclei;

(ii) The Coulomb energy coefficient was determined from the empirical value of the radii of radioactive nuclei

$$a_3 = \frac{3}{5}\frac{e^2}{r_0} = 0.58 \text{ MeV};$$

(iii) The symmetry energy coefficient $a_4 = 19.5$ MeV was defined in such a way that the most stable nucleus with $A = 200$ had charge $Z = 80$.

It was immediately noticed [2, 3] that formula (1) describes the nuclei with even Z and N. The nuclei with odd A have larger masses and, consequently, lower binding energies. The Bethe–Weizsácker formula described the dependence of the binding fraction $\varepsilon(A) = E_{\text{bind}}(A)/A$ on the mass number A and provided the means to explain the process of nuclear fission. The liquid-drop model made it possible to describe the excited states of nuclei as surface oscillations. However, the presence of "magic" N and Z values ($N, Z =$ 2, 8, 20, 28, 50, 82, and 126), which increased the stability of the corresponding atomic nuclei in comparison with their neighboring nuclei, and quantum properties, such as nuclear spin and parity, were explained only after the one-particle shell model was introduced [4].

The interaction of nucleons within a nucleus may be presented as a sum of the mean self-consistent field and the residual interaction. In the simplest one-particle shell model, nucleons travel independently of each other in the self-consistent field of a common center of force. The residual interaction is taken to be negligibly small and is ignored. The shell model of a nucleus was proposed by analogy with the model of the electron shells of an atom, as both nuclei and atoms exhibit a certain "periodicity" of their properties that may be explained by the filling of shells [3]. Strongly bound systems, such as an alpha particle and a ^{16}O nucleus may be presented as completely filled s- and p-shells. Solving the Schrödinger equation for a centrally symmetric oscillatory potential, one obtains the following nuclear shell filling numbers for nucleons of the same type: 2, 8, 20, 40, 70, and 112. The sequence of filling number changes is altered in a spherical potential with a radial dependence of the form of an infinite rectangular well: 2, 8, 20, 34, 40, 58, 92, and 132. This representation made it possible to explain the increased stability of systems with 2, 8, or 20 neutrons (or protons) [3].

The introduction of the spin–orbit interaction $V_{LS}(\mathbf{L} \cdot \mathbf{S})$ into a self-consistent field made it possible to determine the theoretical basis for the emergence of the experimentally derived magic numbers 28, 50, 82, and 126 and to correctly reproduce the quantum properties of ground and certain excited states of nuclei that differ from the magic ones by a single nucleon [4]. The resultant Hamiltonian of the shell model is a sum of one-particle Hamiltonians:

$$H_0 = \sum_{i=1}^{A} [T_i + V(r_i) + V_{LS}(\mathbf{L} \cdot \mathbf{S})], \quad (2)$$

where T_i is the kinetic energy of the ith nucleon and $V(r_i)$ is the mean self-consistent potential. The eigenvalue problem resolves itself to a set of independent one-particle Schrödinger equations:

$$[T_i + V(r_i) + V_{LS}(\mathbf{L} \cdot \mathbf{s})]\psi_i(\mathbf{r}_i) = \epsilon_i \psi_i(\mathbf{r}_i), \quad (3)$$

where $\psi_i(\mathbf{r}_i)$ and ϵ_i are the eigen wavefunction and energy of the ith nucleon. The complete wavefunction of a nucleus is an antisymmetrized product of one-particle wavefunctions, and the energy of a nucleus is a sum of one-particle nucleon energies:

$$E = \sum_{i=1}^{A} \epsilon_i.$$

The ground state of doubly magic nuclei in the one-particle shell model should have zero spin J and positive parity P ($J^P = 0^+$). This agrees with the experimental data. More than 800 known even–even nuclei are peculiar in that all of them have their ground states with spin and parity $J^P = 0^+$. This fact is the most striking evidence that the residual interaction plays an important role and leads to pairing of nucleons of the same type within an atomic nucleus.

The tendency of particles with spin $s = 1/2$ to form bound pairs with total momentum $J = 0$ is observed in

various many-fermion systems. For example, this effect lies in the basis of the description of superconduction in solid-state physics [5, 6]. The interacting fermions in this case are electrons that form Cooper pairs. Since Cooper pairs have integer spins, they are not governed by the Pauli principle and the system manifests certain properties (superfluidity) that are characteristic of many-particle bosonic systems. The theory of pair correlations of a superconducting type in atomic nuclei was constructed in [7–9] and set the stage for extensive studies of the nuclear structure based on a semimicroscopic approach.

Various properties of a nucleus that are not reproduced by the shell model are indicative of the presence of the nucleon pairing effect (e.g., see the discussion in [10–13]). The following facts suggest that the forces of identical nucleon pairing play a significant role in nuclear dynamics.

The ground states of all even–even nuclei have total momentum $J^P = 0^+$.

The composition of the nuclei. It follows from the analysis of the atomic nuclei chart that the most energetically favorable states are nuclei configurations with an even number of nucleons of the same type:

(i) Only four stable isotopes ($^2_1$H, $^6_3$Li, $^{10}_5$B, and $^{14}_7$Ne) with odd proton and neutron numbers are known;

(ii) Only a single stable isobaric nucleus is found for a given odd mass number A; and

(iii) Two or more stable isobaric nuclei with even proton and neutron numbers Z and N (even–even nuclei) may exist for a given even mass number A.

The even–odd effect. Systematic studies of binding energies $E_{\text{bind}}(A)$ show that the following rule is fulfilled for nuclei with odd mass numbers A:

$$E_{\text{bind}}(A) < \frac{1}{2}(E_{\text{bind}}(A-1) + E_{\text{bind}}(A+1)). \qquad (4)$$

In the scientific literature, this effect is called the even–odd staggering (EOS) of binding energy. Figure 2 shows the dependence of the binding energy in isobaric nuclei with $A = 132$ on the nucleus charge. It is seen clearly that the binding energies are split into three groups of nuclei: the ones with even A (even N and Z), the ones with odd A (even N and odd Z or odd N and even Z), and nuclei with even A and odd N and Z. The binding energies of even–even and odd–odd nuclei differ by ~2 MeV. The dependence of the binding energy of a nucleus with an odd A number is located between these dependences (the dashed line in Fig. 2 corresponds to the averaged dependence on Z for nuclei with $A = 131$ and $A = 133$). The magnitude of the EOS effect is defined as the deviation of the experimental binding energy value $E_{\text{bind}}(N, Z)$ from

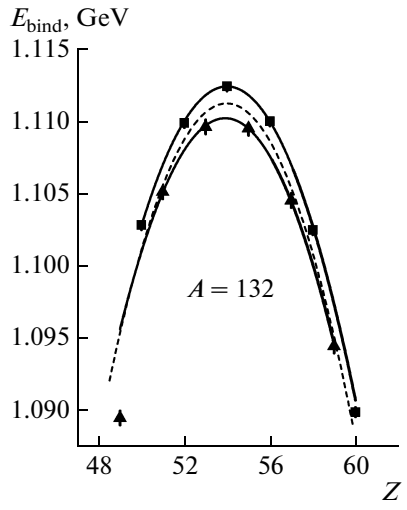

Fig. 2. Dependence of the binding energy of isobaric nuclei with $A = 132$ on nucleus charge Z. Squares denote the binding energy values in nuclei with even numbers N and Z, while triangles correspond to odd–odd N and Z. The dashed line corresponds to the averaged values for $A = 131$ and $A = 133$. Experimental data were taken from [14].

the averaged binding energy value for neighboring nuclei:

$$\Delta_n(N, Z) = E_{\text{bind}}(N, Z) - \frac{1}{2}[E_{\text{bind}}(N-1, Z) + E_{\text{bind}}(N+1, Z)] \qquad (5)$$

(if an odd A number is obtained by adding (subtracting) a neutron) or

$$\Delta_p(N, Z) = E_{\text{bind}}(N, Z) - \frac{1}{2}[E_{\text{bind}}(N, Z-1) + E_{\text{bind}}(N, Z+1)] \qquad (6)$$

(if an odd A number is obtained by adding (subtracting) a proton).

The EOS effect amounts to about 1 MeV in the $A = 130–140$ range.

The even–odd effect is manifested more clearly in the dependence of the nucleon separation energy on mass number A. The neutron separation energy (B_n) equals the following:

$$B_n(N, Z) = M(N-1, Z) + m_n - M(N, Z) = E_{\text{bind}}(N, Z) - E_{\text{bind}}(N-1, Z). \qquad (7)$$

Figure 3 shows the dependences $B_n(A)$ in calcium $^{35–58}$Ca, tin $^{100–138}$Sn, and lead $^{179–220}$Pb isotopes. The clearly manifested sawtooth nature of the dependence points at the pairing interaction between nucleons. The separation energy is increased due to the additional attraction of a pair of neutrons in the case of an even neutron number.

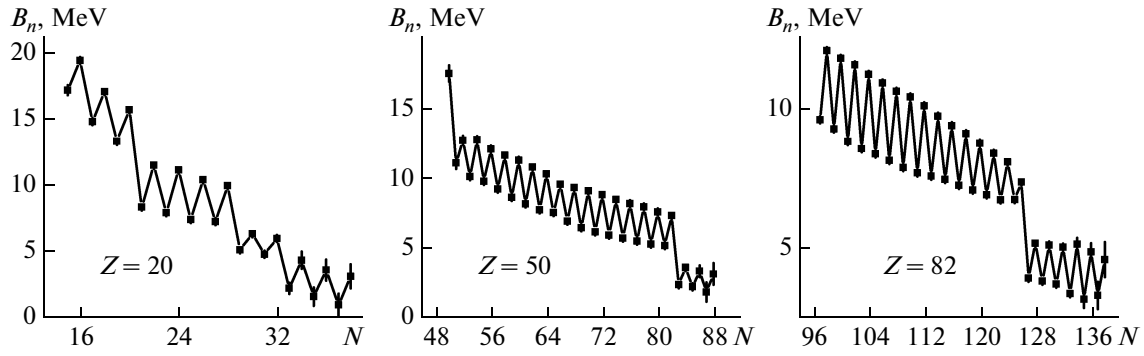

Fig. 3. Dependence of the neutron separation energy (B_n) on neutron number N in Ca, Sn, and Pb isotopes (experimental data were taken from [14]). The sawtooth dependence $B_n(A)$ is explained by the nucleon pairing effect in atomic nuclei. An increased variation of the neutron separation energy at $N = 20$, 28, 50, 82, and 126 is attributed to the filling of nuclear shells.

Figure 4 shows a schematic representation of an atomic nucleus with even numbers N and Z in the form of a closed doubly magic core ($N - 2$, Z) and two valence neutrons. If these valence neutrons did not interact with each other, the separation energy of a pair of neutrons $B_{nn}(N, Z)$ in the nucleus (N, Z) would be equal to twice the neutron separation energy in the nucleus ($N - 1$, Z). The difference between the energy of separation of two neutrons in the nucleus (N, Z) and the doubled neutron separation energy in the nucleus ($N - 1$, Z) results from the residual interaction of two neutrons $\Delta_{nn}(N, Z)$ in nucleus (N, Z):

$$\Delta_{nn}(N, Z) = B_{nn}(N, Z) - 2B_n(N-1, Z)$$

$$= E_{\text{bind}}(N, Z) - 2E_{\text{bind}}(N-1, Z) + E_{\text{bind}}(N-2, Z) \quad (8)$$

$$= B_n(N, Z) - B_n(N-1, Z).$$

However, since an overall reduction in the separation energy B_n is observed when A is increased (Fig. 3), the following averaged value would be more realistic:

$$\Delta_{nn}(N, Z) = B_n(N, Z) - \frac{1}{2}[B_n(N-1, Z) + B_n(N+1, Z)]. \quad (9)$$

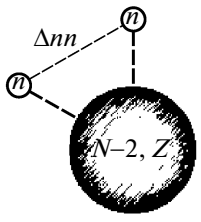

Fig. 4. Residual interaction between a pair of neutrons in nucleus (N, Z). Δ_{nn} is the pairing energy of two neutrons above a closed magic core ($N - 2$, Z).

A comparison of relations (8) and (5) shows that the EOS effect magnitude is actually equal to one half of the pairing value of two neutrons:

$$\Delta_{nn}(N, Z) = 2\Delta_n(N, Z). \quad (10)$$

Energy gap. At energies lower than 1.5 MeV, the spectra of even–even nuclei exhibit a significantly lower number of excited states than the spectra of even–odd nuclei. The majority of these levels have a collective nature and belong to rotational or vibrational spectra.

Figure 5 shows the spectra of the low-lying states of nuclei with even and odd A using the example of calcium $^{42-45}$Ca isotopes. The lowest excited states in even–even isotopes ^{42,44}Ca are located in the energy region $E^* > 1$ MeV, while the lowest excited states in odd isotopes ^{43,45}Ca lie at 373 and 174 keV. This discrepancy may be explained if one takes into account the fact that the bond between paired nucleons has to be severed in order to form the lowest one-particle states in an even–even nucleus.

Moments of inertia. The moments of inertia of even–even nuclei calculated theoretically within the framework of the independent particle model are 2–3 times higher than the experimental values. In addition to this, the moments of inertia of odd nuclei are significantly higher than the moments of inertia of neighboring even–even nuclei and the difference is many times greater than the contribution from a single additional nucleon. If the pairing effects are taken into account, the theoretical values come into agreement with the experimental ones. This is indicative of the presence of a superfluid state of nuclear matter.

Deformations. In the independent particle model, spherical ground states exist only in the nuclei with completely filled shells. All the nuclei with incomplete shells are deformed. However, it follows from the experimental data that the nuclei in the vicinity of magic nuclei also have spherical ground states. The transition to an ellipsoid shape occurs when about a quarter of the

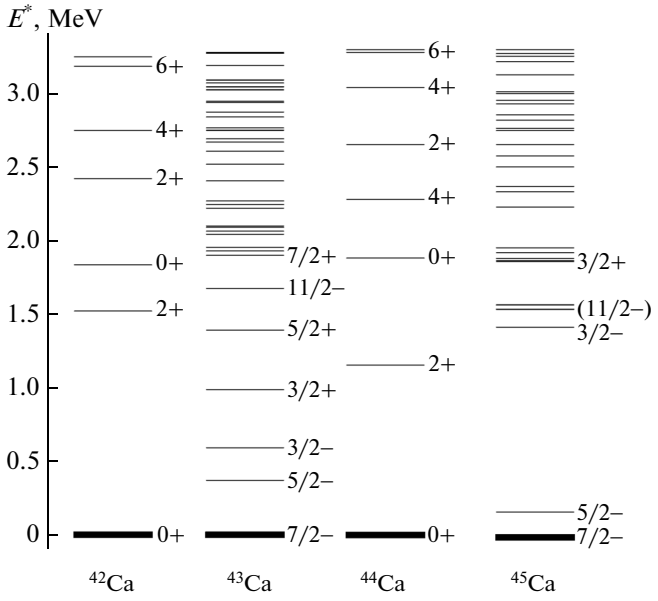

Fig. 5. Spectra of the excited states of calcium $^{42-45}$Ca isotopes. Experimental data were taken from [15].

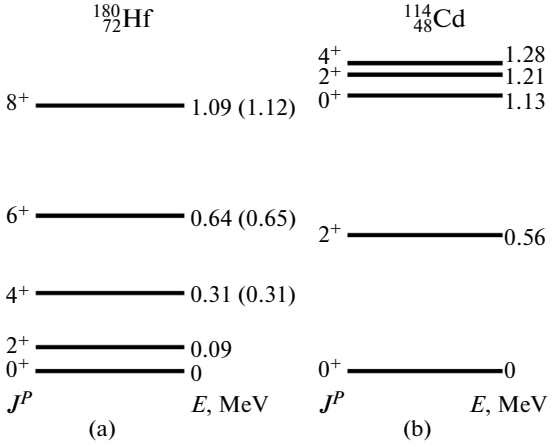

Fig. 6. Examples of spectra of low-lying excited states of different nature. Left panel: the rotational spectrum of ^{180}Hf. The positions of levels calculated within the framework of the rigid rotator model and normalized to the energy of the first level 2^+ are given in brackets. Right panel: the spectrum of quadrupole oscillations of ^{114}Cd. Experimental data were taken from [15].

vacancies in the last shell become filled. As the shell is filled further, the deformation rapidly grows stronger and is maximized when the shell is half filled.

Low-lying 2^+ states. It is not possible to describe the low-lying 2^+ levels in nuclei in the vicinity of magic numbers within the framework of the shell model without pairing. These levels are in most cases described as quadrupole oscillations in the nucleus. This also points to the presence of strong correlations between nucleons.

If the 2^+ levels are to be interpreted as a manifestation of vibrational or rotational degrees of freedom, the spectrum of a nucleus should contain a set of excited states with a certain sequence of spin and parity J^P values and a certain ratio between the nucleus excitation energies. Figure 6 shows two typical examples of spectra of a collective nature: a rotational one and a vibrational one. Each spectrum has a certain sequence of levels and a distinctive ratio between the excitation energies.

Figure 6a shows the spectrum of rotational states of ^{180}Hf. In the case of a rotational spectrum, the nucleus excitation energy is proportional to $J(J+1)$, and the distance between the levels increases with J. The experimental excitation energy values corresponding to different levels are shown on the right and the results of calculations within the framework of the simplest rigid rotator model normalized to the energy of the first excited state $E(2^+) = 93$ keV are put in brackets. It can be seen that the relationship $E(4^+)/E(2^+) = (4 \times 5)/(2 \times 3) = 3.33$ holds true for low-lying excitations.

Figure 6b shows the spectrum of low-lying states of ^{114}Cd. In the case of quadrupole oscillations, the nucleus has an equidistant spectrum with a distinctive sequence of levels. The energies of a group of levels $E(0^+, 2^+, 4^+)$ and the first excited state $E(2^+)$ have a 2 : 1 relationship. Thus, neither the vibrational nor the rotational spectra suggest that the $E(4^+)/E(2^+)$ ratio is significantly lower than 2. Figure 7 shows a chart of the ratio of energies of the first excited states $E(4^+)/E(2^+)$ as a function of Z and N. Dark regions corresponding to $E(4^+)/E(2^+) < 2$ form wide bands located along the magic number lines. It can be seen from Fig. 8 that entire chains of isotopes and isotones fall within the $E(4^+)/E(2^+) < 2$ region. *Excited states of an even parity 2^+ and 4^+ and a non-rotational and non-vibrational nature are present in the nuclei that are located in the vicinity of magic nuclei.* As will be shown below, these states also have a collective nature resulting from nucleon pairing in the nuclei that have pairs of identical nucleons in the outer shell.

1. ESTIMATING THE PAIRING ENERGY VALUE USING THE EXPERIMENTAL DATA ON NUCLEAR-BINDING ENERGIES

The Bethe–Weizsácker formula (1) for a mass surface reproduces the binding energy values of even–even nuclei well. The correction for the even–odd (EOS) effect is defined by the pairing interaction energy and is introduced in the following way:

$$E_{\text{pair}} = \begin{cases} +\delta(A) & \text{when } Z \text{ is even and } N \text{ is even} \\ 0 & \text{when } A \text{ is odd} \\ -\delta(A) & \text{when } Z \text{ is odd and } N \text{ is odd.} \end{cases} \quad (11)$$

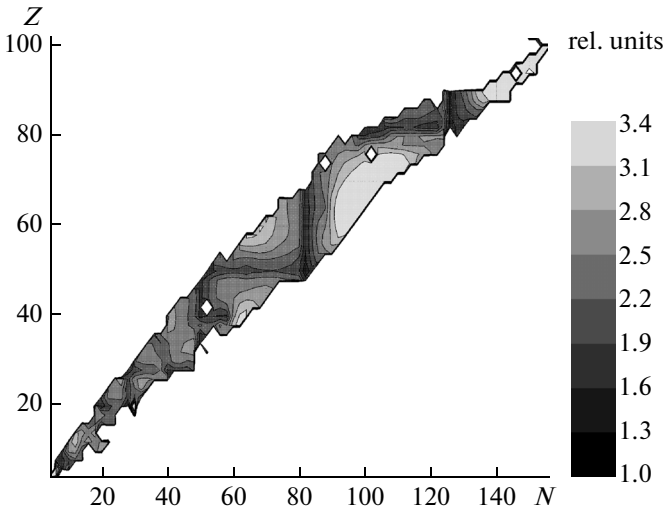

Fig. 7. Ratio of energies of the first excited states with $J^P = 4_1^+$ and $J^P = 2_1^+$. The chart is plotted based on the experimental data taken from [16].

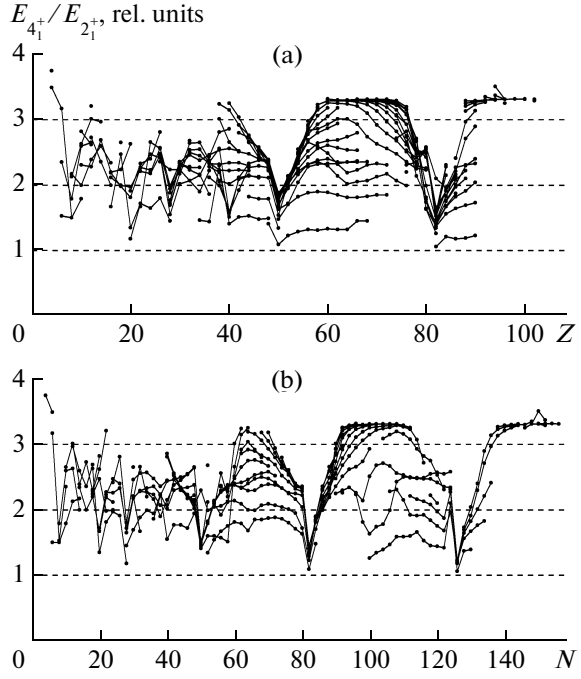

Fig. 8. Ratio of energies of the first excited states with $J^P = 4_1^+$ and $J^P = 2_1^+$ as a function of (a) the proton number Z (lines connect isotones with N = const) and (b) the neutron number N (lines connect isotopes with Z = const). Experimental data were taken from [16].

The parameters of analytical function $\delta(A)$ (11) are determined by fitting the experimental values of the even–odd effect Δ_n (5) and Δ_p (6).

The determination of Δ_n and Δ_p is based on the assumption that the masses of nuclei exclusive of the pairing effect are well described by a smooth function of Z and N. The even–odd (EOS) effect magnitude Δ_n calculated based on three experimental binding energy values is then equal to the following:

$$\Delta_n^{(3)}(N, Z) = E_{\text{bind}}(N, Z) - \frac{1}{2}[E_{\text{bind}}(N-1, Z) + E_{\text{bind}}(N+1, Z)] = \frac{1}{2}[B_n(N, Z) - B_n(N+1, Z)]. \quad (12)$$

However, this linear interpolation does not take into account the mass surface curvature and it systematically overestimates the EOS magnitude.

The authors of [17] proposed a modified formula that is averaged over four binding energy values. For an even neutron number,

$$\Delta_n^{(4)}(N, Z) = \frac{1}{4}[E_{\text{bind}}(N-2, Z) - 3E_{\text{bind}}(N-1, Z) + 3E_{\text{bind}}(N, Z) - E_{\text{bind}}(N+1, Z)] = \frac{1}{2}\left[B_n(N, Z) - \frac{1}{2}[B_n(N-1, Z) + B_n(N+1, Z)]\right], \quad (13)$$

where $B_n(N, Z)$ is the neutron separation energy in nucleus (N, Z) (7). Relationship (13) is taken with an opposite sign if the neutron number N is odd. For an even proton number,

$$\Delta_p^{(4)}(N, Z) = \frac{1}{4}[E_{\text{bind}}(N, Z-2) - 3E_{\text{bind}}(N, Z-1) + 3E_{\text{bind}}(N, Z) - E_{\text{bind}}(N, Z+1)] = \frac{1}{2}\left[B_p(N, Z) - \frac{1}{2}[B_p(N, Z-1) + B_p(N, Z+1)]\right], \quad (14)$$

$$B_p(N, Z) = E_{\text{bind}}(N, Z) - E_{\text{bind}}(N, Z-1).$$

Relationship (14) is also taken with a minus sign if Z is odd.

Expression (13) essentially gives $\Delta_n^{(3)}(N, Z)$ averaged over nuclei (N, Z) and $(N-1, Z)$ and in effect compensates for the systematic error:

$$\Delta_n^{(4)}(N, Z) = \frac{1}{2}(\Delta_n^{(3)}(N, Z) + \Delta_n^{(3)}(N-1, Z)).$$

Figure 9 shows schemes for calculating the even–odd EOS effect using three or four nuclear binding energy values E_{bind} and presents parabolae that correspond to the binding energies in even–even (upper curve) and odd–odd (lower curve) isotopes. The dashed line corresponds to nuclei with odd A. It can be seen that the mass surface curvature produces a systematic error in determining the distance between

even–even and odd–odd surfaces if the calculation is done according to formula (12) with the use of three $E_{\text{bind}}\ \Delta_n^{(3)}$ values. The deviation that results from the mass surface curvature is partially compensated if the calculation is done according to formula (13) with the use of four $E_{\text{bind}}\ \Delta_n^{(4)}$ values.

Since the determination of $\Delta_{n,p}$ from the experimental data is used primarily for obtaining the analytical dependences of the pairing energy on the number of nucleons, the authors of certain recent papers applied even stronger smoothing using formulas that take five [18–20] or six [21] experimental binding energy values into account. An increase in the number of E_{bind} values that are used produces no significant influence on the EOS calculation result; however, the expansion of the experimental data range while moving away from the stable nuclei region may require the use of nuclear-binding energy values with significant errors.

Various analytical dependences of function $\delta(A)$ are known. Experimental data sets were at first fitted with power-law dependences $\delta(A) = a/A^b$. Dependences $A^{-3/4}$ [10, 12] and $A^{-1/2}$ [11, 17] became widely used. The authors of [22] made a comparison between dependences $\delta(A) = 140/A$, $\delta(A) = 36/A^{3/4}$, and $\delta(A) = 10/A^{1/2}$ and showed that function $\delta(A) = 12/A^{1/2}$ produced a slightly better description of the experimental data that were available then (in 1953). As new experimental data on nuclei away from the stability line are gathered, new estimates of parameters of the formula for the nuclear binding energy are presented. In order to take the alteration of the ratio between the proton and neutron numbers into account, the dependence on the relative neutron excess in the nucleus [21, 23–25] is introduced into the pairing-energy parameterization, or the EOS effect is parameterized individually for protons and neutrons [18, 19, 26]. The efforts to take microscopic effects into account and describe a maximally wide range of recent experimental data led to the development of various models that describe the entire set of experimentally determined nuclei masses with an accuracy of 300–600 keV [26–28]. A comparative review of different approaches was given in [29]. Dependence $A^{-1/3}$ is most frequently used as a basic power-law dependence in analytical formulae for the pairing energy.

Figure 10 shows the experimental EOS effect magnitudes $\Delta_{n,p}^{(4)}$ (13, 14) as functions of A. The experimental data spread allows one to use various power-law dependences with equal facility to take into account the correction associated with nucleon pairing in the determination of the nuclear binding energy in the region of nuclei with $A > 50$.

It can be seen from (11) that the additional (with respect to an even–even configuration) energy of an odd–odd nucleus equals $\Delta_p + \Delta_n \approx 2\Delta$ [17]. Consequently, the pairing energy of two nucleons of the same type is defined as follows:

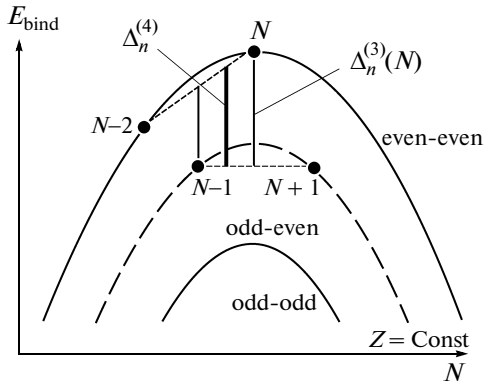

Fig. 9. Scheme for calculating the EOS (the distance between parabolae with even and odd mass numbers A) with the use of three ($\Delta_n^{(3)}$) experimental binding energy values (12) of four ($\Delta_n^{(4)}$) binding energy values (13) .

$$\Delta_{nn}(N, Z) = 2\Delta_n^{(4)} = B_n(N, Z) - \frac{1}{2}(B_n(N-1, Z) + B_n(N+1, Z)), \quad (15)$$

$$\Delta_{pp}(N, Z) = 2\Delta_p^{(4)} = B_p(N, Z) - \frac{1}{2}(B_p(N, Z-1) + B_p(N, Z+1)). \quad (16)$$

These definitions match the equation for Δ_{nn} (9). Figure 11 shows the dependences of pairing energies of two neutrons $\Delta_{nn}(N, Z)$ (15) in even–even magic nuclei Ca, Sn, and Pb on the neutron number. The shell structure of nuclei is clearly manifested in these pairing energies. The pairing energy Δ_{nn} maxima that are found at $N = 20$, 28, 82, and 126 correspond to completely filled neutron shells of atomic nuclei.

2. NUCLEON PAIRING AT SHELL J

The issue of the successive filling of nuclear shells has been discussed in detail in a number of monographs (e.g., [4, 11, 12, 30]).

The effect of the pairing of two nucleons arises as a result of the short-range attractive nucleon–nucleon interaction. A state with an overall total momentum $J = 0$ is more energetically favorable for two nucleons of the same type at subshell j with a given $j_1 = j_2 = j$. This can be seen from the spatial distribution of density of states shown schematically in Fig. 12. It is evident that the distribution density overlap of two nucleons is maximized at $\theta_{12} = 0$, π (i.e., when $|m_j|$ are equal). Since the Pauli principle forbids states with

$\theta_{12} = 0$ ($m_{j_1} = m_{j_2}$), only the combination with $\theta_{12} = \pi$ ($m_{j_1} = -m_{j_2}$) is viable. This implies pairing with total momentum $J = 0$.

The wavefunction of two nucleons in a spherically symmetric potential may be written down in the following form:

$$\Psi(l_1 l_2 : LM, ST) = \sum_{m_1 m_2} \psi_{n_1 l_1 m_1}(\mathbf{r}_1)\psi_{n_2 l_2 m_2}(\mathbf{r}_2)\chi(\mathbf{s}_1\mathbf{s}_2 : S)\xi(\tau_1\tau_2 : T), \quad (17)$$

where $\psi_{nlm}(\mathbf{r}) = \frac{1}{r} R_{nl}(r) Y_{lm}(\theta, \varphi)$ is the spatial one-particle wavefunction, $R_{nl}(r)$ is its radial part, $Y_{lm}(\theta, \varphi)$ are the Spherical Bessel functions, and $\chi(s_1 s_2 : S)$ and $\xi(\tau_1\tau_2 : T)$ are the spin and isospin contributions to the wavefunction. The angular part in the $l_1 = l_2$, $J = 0$, and $M_J = 0$ case is proportional to the Legendre polynomial $P_l(\cos\theta_{12})$:

$$\sum_{m=-l}^{l} (-1)^m Y_{lm}(\theta_1, \varphi_1) Y_{l-m}(\theta_2, \varphi_2) = \frac{2l+1}{4\pi} P_l(\cos\theta_{12}), \quad (18)$$

where θ_{12} is the classical interpretation of an angle between two vectors of nucleon momenta j_1 and j_2 bound in J. This interpretation indicates the extent of wavefunction overlap [31]:

$$\cos\theta_{12} = \frac{J(J+1) - j_1(j_1+1) - j_2(j_2+1)}{2\sqrt{j_1 j_2 (j_1+1)(j_2+1)}}.$$

In the case of a short-range attractive interaction, two nucleons tend to be positioned at an angle that corresponds to the maximum possible spatial distribution overlap.

The attractive δ-potential

$$V(\mathbf{r}_1, \mathbf{r}_2) = -V_0 \delta(\mathbf{r}_1 - \mathbf{r}_2) \quad (19)$$

is a limiting case of a short-range potential and allows one to trace certain patterns characteristic of spectra of two-particle nuclear states for given nucleon configurations. Since the interaction in the simplest case does not depend on spin variables, the spatial and spin variables may be separated. It is convenient to start the analysis from the *LS*-coupling case. The complete wavefunction of two nucleons with orbital momenta l_1 and l_2 $\Psi(l_1 l_2 : LM, ST)$ (17) should be antisymmetric, while the spatial wavefunction of two nucleons should be symmetric: in the δ-interaction case, $\mathbf{r}_1 = \mathbf{r}_2$ and the matrix element with δ-potential in dressings of two antisymmetric functions would equal zero. Therefore, the spin–isospin part should be antisymmetric:

$S = 0$, $T = 1$ correspond to an *nn* or *pp* pair with antiparallel spins, and

$S = 1$, $T = 0$ correspond to an *np* pair with codirectional nucleon spins.

The matrix element of δ-interaction is an integral

$$\langle l_1 l_2 LM | V(\mathbf{r}_1, \mathbf{r}_2) | l_1 l_2 LM \rangle = -V_0 \int \Psi^*_{l_1 l_2 : LM}(1, 2)\delta(\mathbf{r}_1 - \mathbf{r}_2)\Psi_{l_1 l_2 : LM}(1, 2), \quad (20)$$

where $\Psi_{l1l2:LM}(1, 2)$ is a symmetric wavefunction

$$\Psi_{l_1 l_2 : LM}(1, 2) = \frac{1}{\sqrt{2}} \sum_{m_1 m_2} (l_1 m_1 l_2 m_2 | LM) \times (\psi_{n_1 l_1 m_1}(\mathbf{r}_1)\psi_{n_2 l_2 m_2}(\mathbf{r}_2) + \psi_{n_2 l_2 m_2}(\mathbf{r}_1)\psi_{n_1 l_1 m_1}(\mathbf{r}_2)) = \sqrt{2}\frac{R_{n1l1}(r)R_{n2l2}(r)}{r^2} \times \sum_{m_1 m_2} (l_1 m_1 l_2 m_2 | LM) Y_{l_1 m_1}(\theta, \varphi) Y_{l_2 m_2}(\theta, \varphi). \quad (21)$$

Taking the form of the δ-function in a spherical coordinate system into account

$$\delta(\mathbf{r}_1 - \mathbf{r}_2) = \frac{\delta(r_1 - r_2)}{r_1 r_2}\delta(\cos\theta_1 - \cos\theta_2)\delta(\varphi_1 - \varphi_2),$$

we obtain the following for integral (20):

$$\frac{(2l_1+1)(2l_2+1)}{4\pi}\begin{pmatrix} l_1 & l_2 & L \\ 0 & 0 & 0 \end{pmatrix}^2 \int \frac{R^2_{n_1 l_1}(r) R^2_{n_2 l_2}(r)}{r^2} dr. \quad (22)$$

It follows directly from relationship (22) that the sum $l_1 + l_2 + L$ should, in accordance with the properties of coefficients of summation of angular momenta, be even. Therefore, the overall momentum of two nucleons L may take on only even values if two nucleons are situated at the same shell ($l_1 = l_2 = l$, $n_1 = n_2 = n$). The energy shift ΔE_L of a state with a certain L (an increase in the nuclear binding energy in the presence of a residual δ-potential) equals

$$\Delta E_L = -(2l+1)^2 \begin{pmatrix} l & l & L \\ 0 & 0 & 0 \end{pmatrix}^2 V_0 F_0(nl), \quad (23)$$

where $F_0(nl)$ is a radial integral

$$F_0(nl) = \frac{1}{4\pi}\int \frac{R^4_{nl}(r)}{r^2} dr.$$

If $L = 0$, relationship (23) is simplified:

$$\Delta E_0 = -(2l+1) V_0 F_0(nl).$$

The maximum energy shift is found at $L = 0$ and is increased with increasing nucleon orbital momentum l.

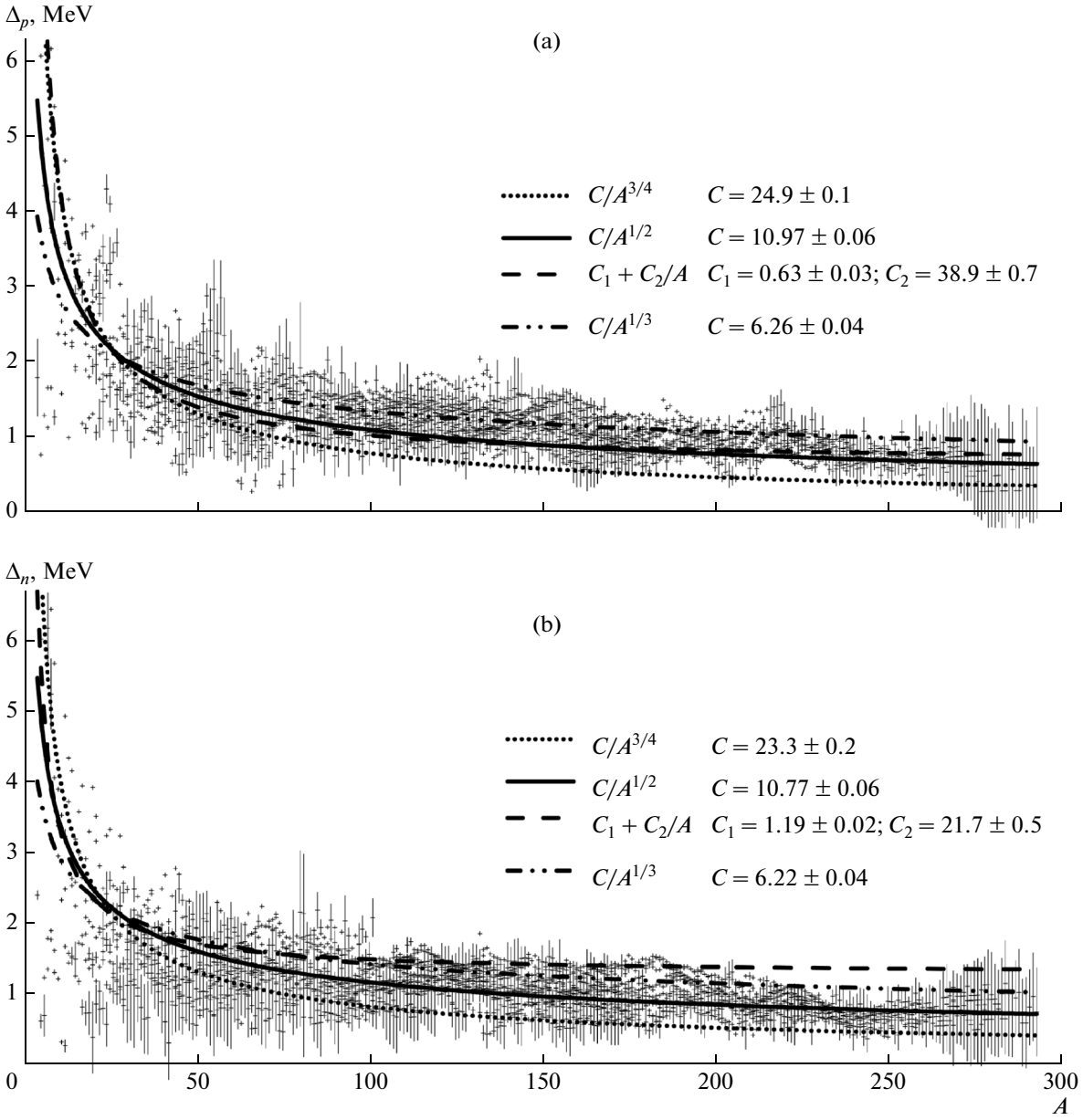

Fig. 10. Different analytical dependences approximating the EOS effect. Upper panel: $\Delta_p^{(4)}$ values are determined using the experimental data from [14], and dotted, solid, dash-and-dot, and dashed curves correspond to analytical dependences $\delta = C/A^{-3/4}$, $\delta = C/A^{-1/2}$, $\delta = C/A^{-1/3}$, and $\delta = C_1 + C_2/A$, respectively. The parameters were determined by approximating the experimental data. Lower panel: the same for $\Delta_n^{(4)}$.

Energy shifts at $L \neq 0$ and large $l \gg L$ are described by the following relationship [32]:

$$\frac{\Delta E_L}{\Delta E_0} \sim \left(\frac{(L-1)!!}{L!!}\right)^2. \quad (24)$$

The characteristic spectrum of states of the $(ll : LM)$ configuration is shown in Fig. 13. As expected, the state with $L = 0$ is the most sensitive to the short-range interaction, while other levels are shifted only slightly. As L is increased, the energy shift between levels tends toward zero. The ratio of energies $E(4^+)/E(2^+)$ in the spectrum of excited states of a nucleus (where the reference energy is taken to be equal to the ground state energy $E_{gs}(J = 0)$) is, contrary to the rotational and vibrational states, lower than 2:

$$\frac{E(4^+)}{E(2^+)} = \frac{1 - \Delta E_4}{\Delta E_2} = \frac{55}{64} \cdot \frac{4}{3} = 1.15.$$

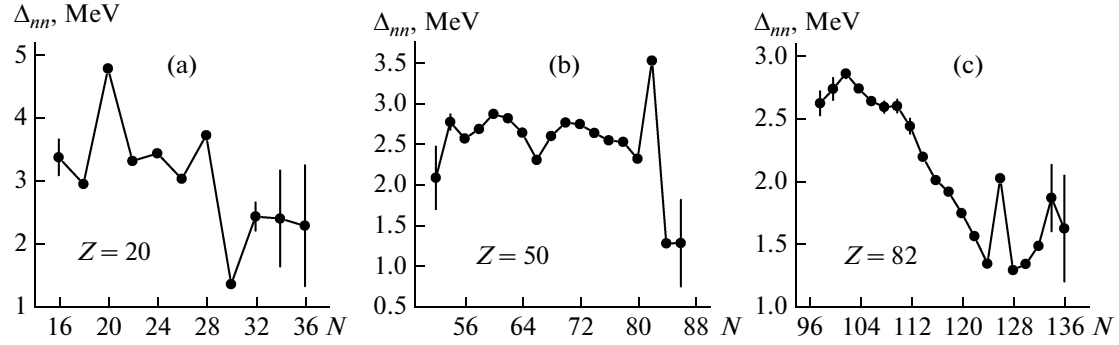

Fig. 11. Neutron pairing energies Δ_{nn} in even–even (a) Ca ($Z = 20$), (b) Sn ($Z = 50$), and (c) Pb ($Z = 82$) isotopes. The pairing energy Δ_{nn} maxima found at $N = 20$, 28, 82, and 126 correspond to completely filled neutron shells. The values of Δ_{nn} were determined using the data from [14].

In passing to the *jj* coupling, the expression for energy shift at $T = 1$ is obtained by applying the standard angular momenta recoupling procedure:

$$\Delta E_{jj:J}(T = 1) = -\frac{1}{2}V_0F_0(nl)(2j+1)^2\begin{pmatrix} j & j & J \\ 1/2 & -1/2 & 0 \end{pmatrix}^2. \quad (25)$$

The total momentum J runs through even values

$$J^P = 0^+, 2^+, 4^+ \ldots (J^P_{\max} = (2j-1)^+). \quad (26)$$

In the $T = 0$ case (*np* pair), the total momentum takes on odd values, and the energy shift for these values equals the following [30]:

$$\Delta E_{jj:J}(T = 0) = -\frac{1}{2}V_0F_0(nl)(2j+1)^2 \times \begin{pmatrix} j & j & J \\ 1/2 & -1/2 & 0 \end{pmatrix}^2 \left[1 + \frac{(2j+1)^2}{J(J+1)}\right]. \quad (27)$$

The relative energy shift values $\Delta E_J/\Delta E_0$ for *nn* and *pp* pairs ($T = 1$) and j ranging from 5/2 to 13/2 are presented in Table 1. Since the level splitting in a multiplet depends only on the angular part and is defined by the coefficients listed in Table 1, one may obtain the spectrum of low-lying states using an experimental $E(jj : J_{\max})$ value. Figure 14 shows the spectrum of low-lying excited states of ^{210}Po. The experimental excitation energy values [15] are shown on the right. The results of calculating the multiplet energies on the assumption that a pair of protons above the doubly magic ^{208}Pb core is in state $1h_{9/2}$ are put in brackets. The calculation results are in a good agreement with the experimental data. It should be noted that the ground state of a pair of protons $J^P = 0^+$ could be described more precisely as a complex of one-particle configurations with eigenvalue differences that do not exceed ΔE. In the case of ^{210}Po, the main contribution of configuration $(1h_{9/2})^{2\pi}$ is supplemented with significant additions of other states:

$$|^{210}\mathrm{Po}_{\mathrm{g.s.}}\rangle \approx [c_1|(1h_{9/2})^{2\pi}_{J=0}\rangle + c_2|(2f_{7/2})^{2\pi}_{J=0}\rangle + c_3|(1i_{13/2})^{2\pi}_{J=0}\rangle + \ldots]|^{208}\mathrm{Pb}_{\mathrm{g.s.}}\rangle.$$

Thus, the ^{210}Po nucleus in its ground state is not a system of independent particles, but a system of independent particle pairs [13].

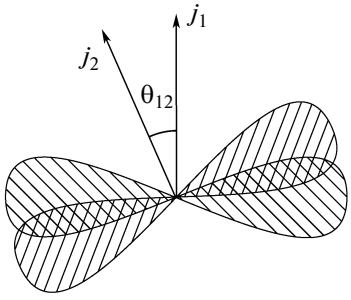

Fig. 12. Schematic representation of the overlap of spatial distributions of wavefunctions of two nucleons in state j_1, j_2. The overlap is maximized at $j_1 = j_2$ and $\theta_{12} = 0, \pi$.

A low magnitude of splitting of levels with $J = 2^+$, 4^+, 6^+, 8^+ of the ^{210}Po ground state multiplet allows one to describe these levels as degenerate states of the one-particle shell model in the pairing interaction approximation. Racah studied the problem of N degenerate states at shell j with a pairing interaction; these studies resulted in the construction of the seniority scheme [33]. The pairing interaction between nucleons in this scheme acts only in the state of maximum correlation of the pair of valence nucleons (i.e., paired particles are particles with the maximum wavefunction overlap, $m_{j_1} = -m_{j_2}$). Since the pairing interaction Hamiltonian acts only on the state with $J = 0$, it is shifted downward in energy and corresponds to the state with seniority $s = 0$ (s is the number

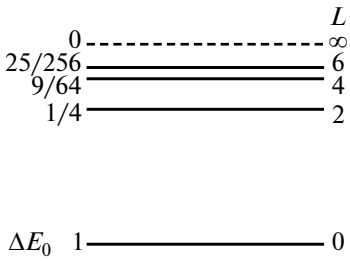

Fig. 13. Spectrum of states of the $(ll : LM)$ configuration. Normalized values of the state energy shift $|\Delta E_L/\Delta E_0|$ calculated in the $l \gg L$ limit (relationship (24)) are shown on the left.

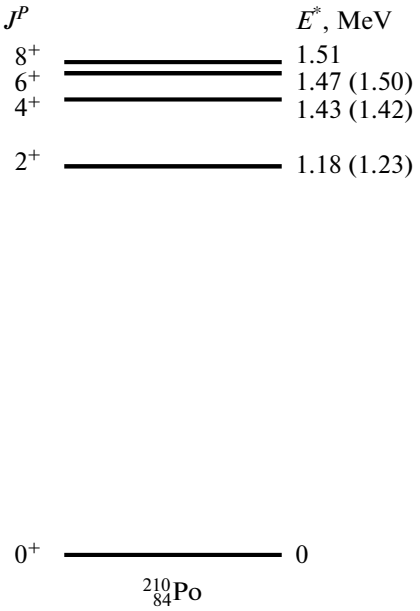

Fig. 14. Spectrum of low-lying excited states of ^{210}Po. The experimental excitation energy values [15] are shown on the right. The results of calculating the energies of the ground state multiplet for the δ-potential normalized to energy $E^*(8^+)$ of the excited state $J^P_{\max} = 8^+$ are put in brackets.

of unpaired particles). The other states are not shifted and have $s = 2$. The pairing interaction spectrum is shown in Fig. 15b. It can be seen that a downward shift of the state with $J = 0$ creates an energy gap between the ground state $J = 0$ and the first excited state $J = 2^+$ of a pair of nucleons in an atomic nucleus.

Further development of the theory of pairing interaction of nucleons is associated with the Bardeen–Cooper–Schrieffer (BCS) model [5] and the Bogoliubov transformations [6]. The basis of eigen wavefunctions in the BCS theory is a set of eigenstates of the Hamiltonian $H_0 + h_{\text{pair}}$ that includes both the shell model Hamiltonian H_0 (2) and the residual pairing interaction h_{pair}. The ground state of even–even nuclei corresponding to this basis has a momentum $J^P = 0^+$ and is a "condensed" state. Since lower "one-particle" excited states are formed upon the pair breakdown, their energy should be higher than 2Δ. Such excitations are called the quasiparticle ones and are formed from particle and hole excitations relative to the ground state of doubly magic nuclei. The energy of a quasiparticle at shell j equals the following:

$$\tilde{\epsilon}_j = \sqrt{\epsilon_j^2 + \Delta^2},$$

where ϵ_j is the one-particle energy in neglect of the residual interaction (relationship (3)). One-particle excited states formed as a result of the pair breakdown in even–even nuclei are two-quasiparticle states (similar to particle–hole states in doubly magic nuclei). Such states lie above the minimum energy 2Δ ($2\tilde{\epsilon}_j$ if $\epsilon_j = 0$).

The energy-gap parameter in the BCS theory is related to the energies of the ground states of the nuclei:

$$\frac{1}{2}(E(A+2) + E(A) - 2E(A+1)) \approx \Delta_{\text{BCS}}.$$

This means that the Δ_{BCS} parameter corresponds to the even–odd EOS effect and its definition matches the definition of the pairing interaction energy E_{pair} in the Bethe–Weizsácker formula. Since the energy gap parameter Δ in the BCS theory should not depend on A, an attempt is made to separate the contributions of the BCS pairing and many-particle effects in the EOS parameterization. The role that the additional contributions to EOS play has been actively discussed [34–37]. The authors of [37] proposed a parameterization

Table 1. Relative energy shift value $\Delta E_J/\Delta E_0$ in the case of a pair of valence protons or neutrons at subshell j

	$J = 0$	2	4	6	8	10	12
$j = 5/2$	1	0.2285	0.0952				
7/2	1	0.2381	0.1169	0.0583			
9/2	1	0.2424	0.1259	0.0746	0.0403		
11/2	1	0.2448	0.1305	0.0823	0.0531	0.0300	
13/2	1	0.2461	0.1333	0.0866	0.0596	0.0403	0.0234

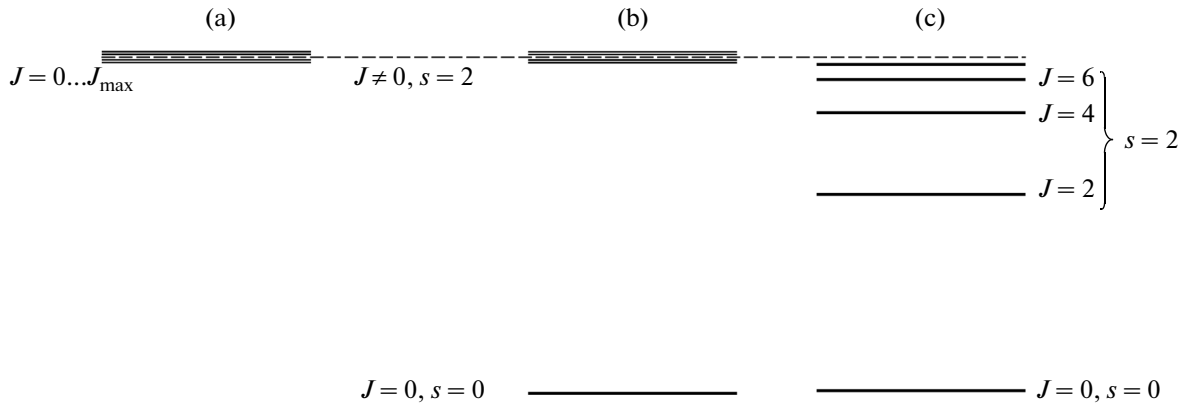

Fig. 15. Spectra of excited states of nuclei with two identical nucleons at shell j (a) in the shell model without the residual pairing interaction, (b) in the seniority scheme with the pairing interaction, and (c) with δ-interaction.

for EOS that takes the form of a sum of two summands:

$$\Delta = C_1 + C_2/A, \tag{28}$$

where the constant C_1 is related to the BCS effect and the contribution inversely proportional to A effectively takes the mean field influence into account. The procedure of fitting the parameters using different experimental data groups and Δ definitions (13) and (14) revealed that the contribution of the BCS pairing interaction to EOS amounts to 75–80% [37]. Figure 10 shows analytical dependence (28) with the values of coefficients C_1 and C_2 determined using the entire set of currently known binding energy values.

3. GROUND STATE MULTIPLETS OF EVEN–EVEN NUCLEI

3.1. Multiplets of Nuclei with a Pair of Neutrons or Protons above a Magic Core

The surface δ-interaction was introduced [30, 38–41] as a simple scheme for calculating the structures of atomic nuclei. A sole adjustable parameter characterizing the interaction strength was determined either by fitting the energy of the first excited state 2^+ or from the EOS effect magnitude fitting [31, 39]. The authors of [42] analyzed nuclei with a pair of nucleons (holes) above a magic core where the δ-interaction parameter $V(\mathbf{r}_1, \mathbf{r}_2) = -V_0(A)\delta(\mathbf{r}_1 - \mathbf{r}_2)$ was determined from an experimental data set based on the excited states of nuclei. Taking into account the dependence $V_0(A) = v_0 A^{-2/3}$ for $A > 20$ (in the case of neutron pairs) and $A > 50$ (in the case of proton pairs), the authors obtained the following values of coefficient v_0:

$$\begin{aligned} v_0(\text{protons}) &= 11.4 \pm 0.9 \text{ MeV}; \\ v_0(\text{neutrons}) &= 10.3 \pm 1.4 \text{ MeV}. \end{aligned} \tag{29}$$

A more complex dependence on $V_0(A)$ was used for light nuclei.

The values of energy $E(J_{\max})^{\text{fit}}$ of levels $|jj : J_{\max} = 2j - 1\rangle$ calculated in [42] using these coefficients are listed in the fourth column of Table 2. The basic configurations of a pair of valence nucleons or holes are listed in the second column (quantum numbers *nlj* are put in brackets, and indices 2π and 2ν indicate the nucleon number and type). It is assumed that the main contribution to the ground state multiplet is provided by the states with a pair of nucleons at a shell that is the closest to the filled core.

The last column of Table 2 lists the pairing energies of nucleons of the same type $E_{\text{pair}} = \Delta_{NN}$ (the nucleon type is indicated in brackets) calculated according to formulas (15) and (16). It can be seen that the ground state multiplet for hole configurations also matches in magnitude the pairing energy of the corresponding nucleons. The excitation energy $E(J_{\max})^{\text{pair}}$ values calculated based on E_{pair} are listed in the fifth column of Table 2. The excitation energies $E(J_{\max})^{\text{pair}}$ agree well with the experimental values. The largest discrepancy is observed in the case of the neutron-excess nucleus ^{76}Ni. The neutron-pairing energy for this nucleus is determined with a significant error: $\Delta_{nn}(^{76}\text{Ni}) = 1.97 \pm 0.76$ MeV.

The use of the experimental value of the pairing energy of two nucleons Δ_{nn} (Δ_{pp}) as the ground state energy shift $E(jj : 0)$ in relationship (25) allows one to refine the structure of the ground-state multiplet. Table 3 presents the spectra of ground-state multiplets for a pair of nucleons in state $j = 9/2$ calculated based on the splitting magnitude ($E(0^+) - E(8^+)$) and the experimental pairing energy value $E_{\text{pair}} = \Delta_{nn}$ (Δ_{pp}). It should be noted that the excitation energies of the ground state multiplet obtained in the second calculation are in a good agreement with the experimental values, including the ones that correspond to levels with $J = J_{\max}$.

Table 2. Splitting of ground state multiplets of nuclei with a doubly magic core and a pair of valence nucleons (holes) of the same type. The basic configurations of a pair of valence nucleons are listed in the second column. $E(J_{max})$ is the excitation energy of level J_{max} (26): $E(J_{max})^{exp}$ are the experimental values taken from [15], $E(J_{max})^{fit}$ are the values from [42], and $E(J_{max})^{pair}$ are the results of calculation in the δ potential approximation based on the pairing energy of two nucleons E^{pair} that was determined using the data from [14]

$^{A}X(N, Z)$	Basic config.	$E(J_{max})^{exp}$, MeV [15]	$E(J_{max})^{fit}$, MeV [42]	$E(J_{max})^{pair}$, MeV	E^{pair}, MeV
^{18}O(10, 8)	$(1d_{5/2})^{2\nu}$	3.555	3.704	3.616	3.996 (*nn*)
^{18}Ne(8, 10)	$(1d_{5/2})^{2\pi}$	3.376	2.517	3.424	3.784 (*pp*)
^{42}Ca(22, 20)	$(1f_{7/2})^{2\nu}$	3.189	3.317	3.137	3.333 (*nn*)
^{42}Ti(20, 22)	$(1f_{7/2})^{2\pi}$	3.043	3.225	2.974	3.158 (*pp*)
^{46}Ca(26, 20)	$(1f_{7/2})^{-2\nu}$	2.974	2.938	2.874	3.052 (*nn*)
^{50}Ti(28, 22)	$(1f_{7/2})^{2\pi}$	3.199	3.175	3.122	3.315 (*pp*)
^{54}Fe(28, 26)	$(1f_{7/2})^{-2\pi}$	2.949	2.934	2.863	3.042 (*pp*)
^{76}Ni(48, 28)	$(1g_{9/2})^{-2\nu}$	2.420	2.996	1.888	1.967 (*nn*)
^{92}Mo(50, 42)	$(1g_{9/2})^{2\pi}$	2.761	2.764	2.723	2.837 (*pp*)
^{98}Cd(50, 48)	$(1g_{9/2})^{-2\pi}$	2.428	2.539	2.516	2.622 (*pp*)
^{130}Sn(80, 50)	$(1h_{11/2})^{-2\nu}$	2.435	2.312	2.264	2.334 (*nn*)
^{134}Sn(84, 50)	$(2f_{7/2})^{2\nu}$	1.247	1.497	1.218	1.293 (*nn*)
^{134}Te(82, 52)	$(1g_{7/2})^{2\pi}$	1.691	1.656	1.693	1.798 (*pp*)
^{148}Dy(82, 66)	$(1h_{11/2})^{2\pi}$	2.919	2.393	2.792	2.878 (*pp*)
^{210}Pb(128, 82)	$(2g_{9/2})^{2\nu}$	1.278	1.408	1.247	1.299 (*nn*)
^{210}Po(126, 84)	$(1h_{9/2})^{2\pi}$	1.557	1.558	1.528	1.593 (*pp*)

Table 3. Ground state multiplets of ^{210}Po$(1h_{9/2})^{2\pi}$ and ^{210}Pb$(2g_{9/2})^{2\nu}$. Experimental data were taken from [15]

J^P	$E_{JP}(^{210}\text{Po})$, MeV			$E_{JP}(^{210}\text{Pb})$, MeV		
	exp. [15]	calculated based on $E(8^+)$	calculated based on Δ_{pp}	exp. [15]	calculated based on $E(8^+)$	calculated based on Δ_{nn}
8^+	1.56		1.53	1.28		1.25
6^+	1.47	1.50	1.47	1.20	1.23	1.20
4^+	1.43	1.42	1.39	1.10	1.17	1.14
2^+	1.18	1.23	1.21	0.80	1.01	0.98

3.2. Systematics of Low-Lying Excited States of Atomic Nuclei

We have analyzed the pairing energies of two nucleons and the splitting of nuclei ground state multiplets as functions of filling the valence subshell with proton or neutron pairs. Figures 16–19 show the spectra of low-lying states of even–even nuclei. The core in all the presented isotone and isotope chains is the doubly magic nucleus ^{208}Pb ($Z = 82$, $N = 126$). The multiplet structure for two nucleons is clearly manifested in the considered cases. Figure 16 shows the spectra of isotonic nuclei with $N = 126$ for different proton numbers Z. The isotones are indicated at the bottom of the figure and the basic valence nucleon configurations in the shell model are indicated above the spectra. The proton number at shell $1h_{9/2}$ varies from 2 to 8 (even numbers). The multiplets of ground states (2^+, 4^+, 6^+, 8^+) converging to the proton pairing energy are visible for the nuclei that have proton pairs at shell $1h_{9/2}$. The multiplet structure does not change as proton pairs are added and the multiplet splitting magnitude corresponds to the pairing energy of two protons Δ_{pp} that falls within the range from 1.593 ± 0.003 MeV to 2.09 ± 0.30 MeV. Isotones ^{210}Po, ^{212}Rn, ^{214}Ra, and ^{216}Th are described well by the seniority model in which the structure of the multiplet with seniority $s = 2$ ($J^P = 2^+, 4^+, 6^+, 8^+$) is retained as pairs of nucleons with $j = 9/2$ are added and the states $J^P = 10^+, 12^+$ with an excitation energy of about 3 MeV are observed in the case of four or six protons at the subshell for $s = 4$ [13, 30].

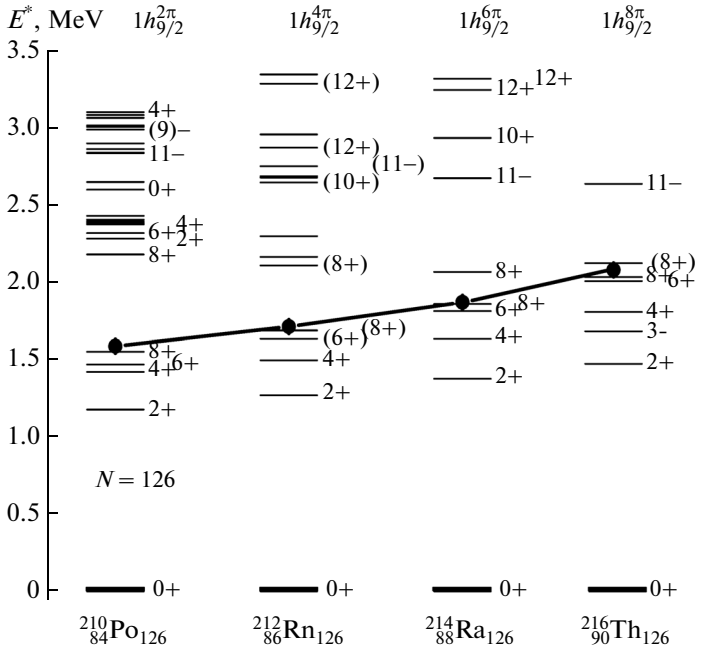

Fig. 16. Pairing energies Δ_{pp} (●) determined using relationship (16) and the data from [14] and the spectra of low-lying states for isotonic nuclei with $N = 126$ and closed neutron shells (experimental data from [15, 16]). The multiplets of ground states (2^+, 4^+, 6^+, 8^+) converging to the proton pairing energy Δ_{pp} are visible for the nuclei having proton pairs at shell $1h_{9/2}$.

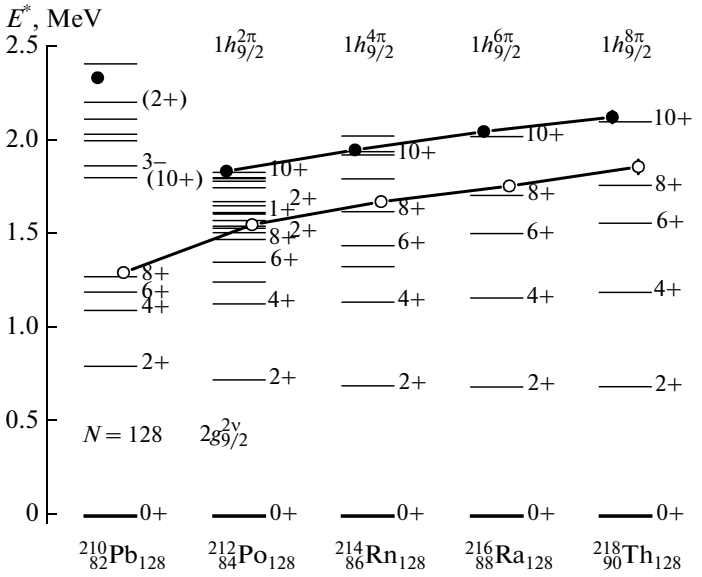

Fig. 17. Pairing energies Δ_{nn} (○) and Δ_{pp} (●) determined using relations (16) and (15) and the data from [14] for isotonic nuclei with $N = 128$ and a pair of neutrons at shell $2g_{9/2}$. In contrast to isotones with $N = 126$ (Fig. 16), the multiplets of ground states (2^+, 4^+, 6^+, 8^+) converge to the neutron pairing energy Δ_{nn} (○). The proton pairing energy corresponds to states 10^+ in the nuclei spectra. The experimental excitation energy values were taken from [15, 16].

The chain of isotonic nuclei with $N = 128$ shown in Fig. 17 corresponds to the core of a doubly magic ^{208}Pb nucleus with a pair of neutrons in state $2g_{9/2}$ above the closed shell added to it. The neutron pair in ^{210}Pb forms the ground state multiplet, whose structure is also discernible in the remaining isotones ^{212}Po, ^{214}Rn,

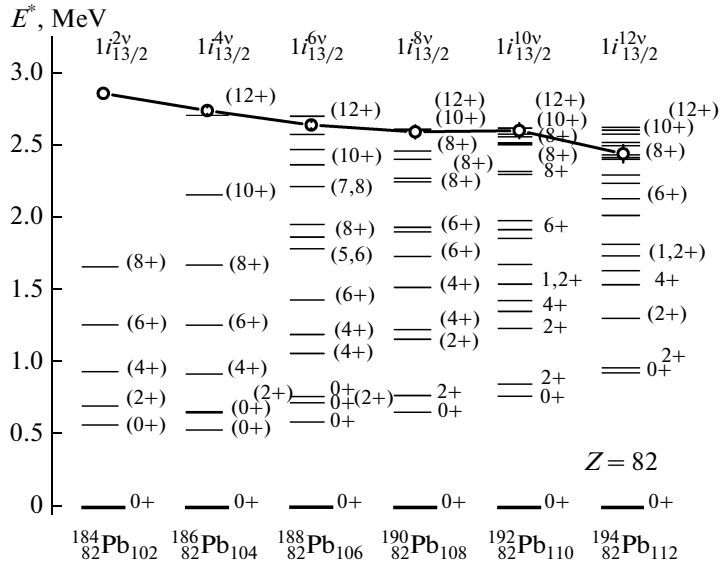

Fig. 18. Manifestations of multiplets of the ground state of neutron pairs at subshell $1i_{13/2}$ (2^+, 4^+, 6^+, 8^+, 10^+, 12^+) of lead isotopes (experimental data from [15, 16]). Neutron pairing energies Δ_{nn} (○) determined using the data from [14] are indicated.

^{216}Ra, and ^{218}Th, with the pairing energy of two neutrons increasing from $\Delta_{nn}(^{210}\text{Pb}) = 1.299 \pm 0.003$ MeV to $\Delta_{nn}(^{218}\text{Th}) = 1.99 \pm 0.06$ MeV and corresponding to state 8^+. This suggests that the configuration of ^{212}Po (and other isotones with $N = 128$) is based on the core of ^{210}Pb and not, as is usually assumed, on the core of ^{210}Po. By analogy with ^{210}Po, level $J^P = 8^+$ in the calculations concerning ^{212}Po [30] was associated with the proton configuration $(1h_{9/2})^2$. However, the correct structure of the yrast band $J = 0^+ - 16^+$ as a coupling of configurations $(1h_{9/2})^{2\pi} \times (2g_{9/2})^{2\nu}$ could not be obtained [30, 43]. The reason lies in the fact that this band of states arises as a result of both the interaction of protons with neutrons and the pairing interaction of identical nucleons. The best match between the calculated structure of ^{212}Po and the experimental data is obtained when the component associated with the alpha-clusterization of nucleons in an atomic nucleus is taken into account [43, 44]. The pairing energy of two protons varies within the range from $\Delta_{pp}(^{212}\text{Po}) = 1.841 \pm 0.007$ MeV to $\Delta_{pp}(^{218}\text{Th}) = 2.13 \pm 0.03$ MeV. The value of Δ_{pp} in ^{212}Po (and in the other isotones in the chain) corresponds to the 10^+ excitation level. This may result from mixing of the multiplet of pairing interaction of two protons with collective excitations. It can be seen that the multiplet structure assumes a shape that is characteristic of a rotational band as the proton number increases. This is indicative of an increasing deformation of the nucleus.

Figure 18 shows the spectra of excited states of even–even lead isotopes $^{184-194}$Pb in which neutron pairs are gradually removed from shell $1i_{13/2}$. Although the spectra have a complex structure and the measurement error is increased when moving away from stable nuclei $^{204,206-208}$Pb towards proton-excess isotopes, the correspondence between the pairing energy of two neutrons Δ_{nn} and the excitation energy of level 12^+ is discernible. The nucleus deformation grows stronger (and the rotational nature of the spectrum is manifested more and more clearly) with decreasing neutron number and increasing distance from the doubly magic nucleus ^{208}Pb. The neutron pairing energy increases from $\Delta_{nn}(^{194}\text{Pb}) = 2.45 \pm 0.06$ MeV to $\Delta_{nn}(^{184}\text{Pb}) = 2.86 \pm 0.04$ MeV.

The pairing effect is manifested more clearly when subshell $2g_{9/2}$ in even–even lead isotopes ^{210,212,214}Pb is filled with neutrons (Fig. 19). The multiplet structure does not change as a neutron pair is added in ^{210,212}Pb nuclei, and the excited state with $J_{\max} = 8^+$ corresponds to the pairing energy of two neutrons Δ_{nn}. By analogy with the addition of proton pairs to $1h_{9/2}$ in isotones with $N = 126$ (Fig. 16), it may be assumed that excited states $J^P = 4^+, 6^+, 8^+$ should be observed in the ^{214}Pb isotope near the neutron pairing energy $\Delta_{nn} = 1.49 \pm 0.08$ MeV.

Figure 20 shows the spectra of low-lying excited states of even–even tin ($Z = 50$) isotopes ranging from ^{120}Sn to ^{130}Sn. The $(1h_{11/2})$ shell is gradually filled with neutrons in these isotopes. The neutron pairing energy Δ_{nn} is reduced from $\Delta_{nn}(^{120}\text{Sn}) = 2.778 \pm 0.001$ MeV to $\Delta_{nn}(^{130}\text{Sn}) = 2.33 \pm 0.02$ MeV and corresponds to excitation levels $J = 10^+$. All the isotopes shown are characterized by a wide energy gap between the ground

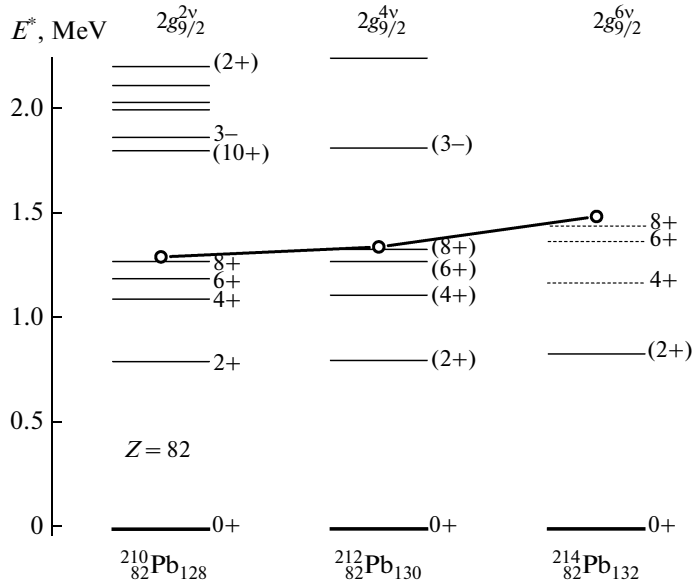

Fig. 19. Multiplets of the ground state of neutron pairs at subshell $2g_{9/2}$ (2^+, 4^+, 6^+, 8^+) of lead isotopes (experimental data from [15, 16]) and neutron pairing energies Δ_{nn} (○) determined using the data from [14].

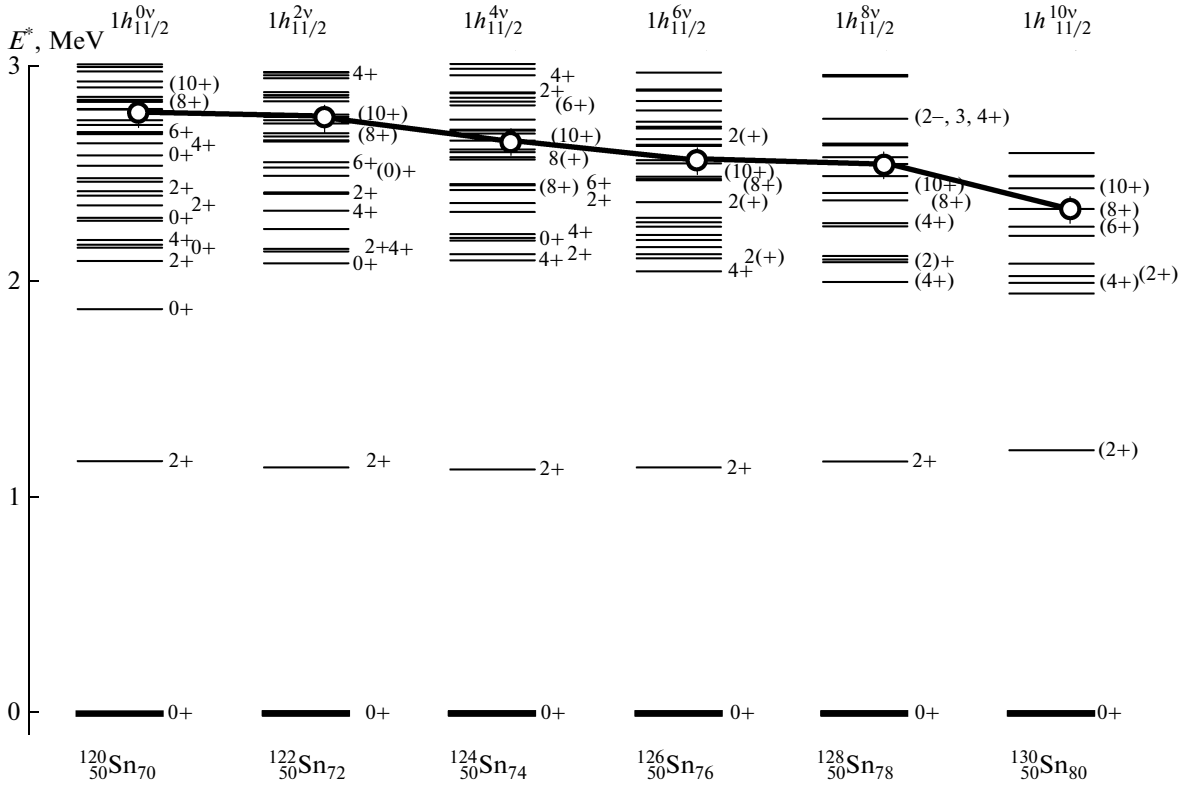

Fig. 20. Multiplets of the ground state of neutron pairs at subshell $1h_{11/2}$ (2^+, 4^+, 6^+, 8^+, 10^+) of tin isotopes (experimental data from [15, 16]). Neutron pairing energies Δ_{nn} (○) were determined using the data from [14].

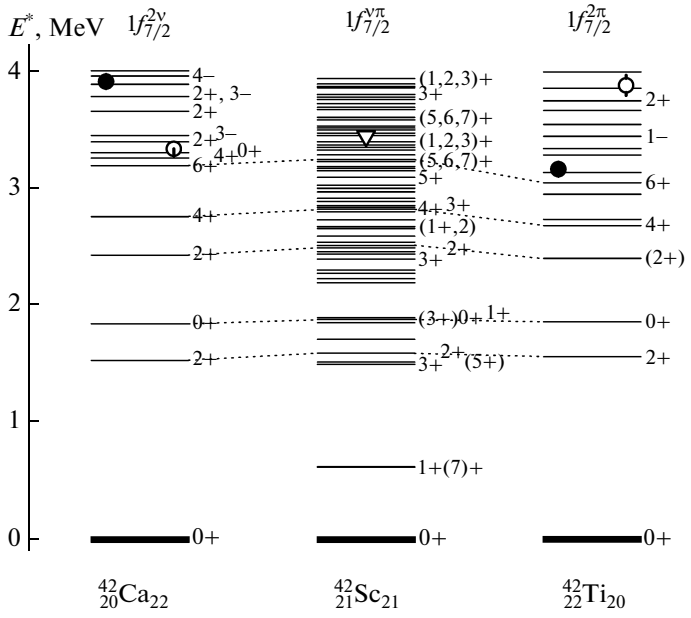

Fig. 21. Pairing energies of nucleons in state $1f_{7/2}$ Δ_{pp} (●) and Δ_{nn} (○) determined using the data from [14] and spectra of low-lying excited states of ^{42}Ca, ^{42}Sc, and ^{42}Ti (experimental data from [15, 16]). Indices above the spectra indicate the basic configurations of nucleon pairs above the doubly magic core. Analog states with $T = 1$ are connected with a dashed line. The *np* pairing energy $\Delta_{np}(^{42}\text{Sc}) = 3.34$ MeV (▽) was determined from the splitting of multiplet $E^*(6^+)$.

state and the first excited one (2_1^+). This may be interpreted as a manifestation of pairing forces and the first excited state 2_1^+ may be treated as a level of the ground state multiplet. On the other hand, relationship $E(4_1^+)/E(2_1^+) \approx 2$ holds true for these Sn isotopes. This is characteristic of vibrational spectra and allows one to interpret the first excited state as single-phonon vibrations. Such an interpretation of this state in effect implies the presence of strong pairing between nucleons [13].

3.3. Pairing np Interaction

The pairing of identical nucleons is usually analyzed. However, the possibility of proton–neutron pairing follows from the charge independence of strong interaction. Such interactions between two protons (V_{pp}), two neutrons (V_{nn}), and a proton and a neutron (V_{np}) should be identical. It is difficult to conduct experimental studies of *np*-pairing, as only a small number of nuclei in which the valence proton and the valence neutron are in the same state above a core with closed shells are known [31, 45]. One such nucleus is that of ^{42}Sc: this isotope has a ^{40}Ca core with one proton and one neutron above it at shell $1f_{7/2}$. Figure 21 shows the spectrum of low-lying excited states of ^{42}Sc and the corresponding spectra of isobaric nuclei ^{42}Ca and ^{42}Ti. The spectrum of excited states of the ^{42}Sc isotope has a more complex structure of its excited states than the spectra of even–even isotopes ^{42}Ca and ^{42}Ti. A sequence of levels with isospin $T = 1$ and even values of spin J (0^+, 2^+, 4^+, 6^+) that corresponds to multiplets of states of isobaric nuclei ^{42}Ca and ^{42}Ti is discernible in the spectrum of ^{42}Sc. Table 4 lists the results of calculating the levels of the $(1f_{7/2})^2$ multiplet using relationship (25) and taking the neutron pairing energy $\Delta_{nn}(^{42}\text{Ca}) = 3.33$ MeV and the proton pairing energy $\Delta_{pp}(^{42}\text{Ti}) = 3.13$ MeV into account. The levels of a multiplet of low-lying analog states in ^{42}Sc with even values of spin J and isospin $T = 1$ were calculated based on the energy $E(6^+) = 3.24$ MeV. In order to reproduce this value for the splitting of the multiplet with $T = 1$, one should assume the value of $\Delta_{np}(T = 1) = 3.44$ MeV. This is close to the averaged value of identical nucleon pairing in neighboring even–even nuclei:

$$\Delta_{np}(^{42}\text{Sc}) = \frac{1}{4}(\Delta_{pp}(^{42}\text{Ca}) + \Delta_{nn}(^{42}\text{Ti}) + \Delta_{nn}(^{42}\text{Ca}) + \Delta_{pp}(^{42}\text{Ti})) = 3.57 \text{ MeV}. \quad (30)$$

According to [17], the energy of proton–neutron pairing in a nucleus should be estimated as $\Delta_{np} = (\Delta_n^{(4)} + \Delta_p^{(4)})$. The *np* pairing value Δ_{np} that were calculated based on the experimental binding energies for an odd–odd nucleus ^{42}Sc equals 2.51 MeV. This value is significantly lower than the splitting of the ground

Table 4. Multiplets of a pair of nucleons in state $1f_{7/2}$ in isobars ^{42}Ca, ^{42}Sc, and ^{42}Ti. Experimental data were taken from [15]. Analog states with $T = 1$ are listed for ^{42}Sc

J^P	$E_{JP}(^{42}\mathrm{Ca})$, MeV		$E_{JP}(^{42}\mathrm{Sc})$, MeV		$E_{JP}(^{42}\mathrm{Ti})$, MeV	
	exp. [15]	calc.	exp. [15]	calc.	exp. [15]	calc.
6_1^+	3.19	3.14	3.24	3.24	3.04	2.97
4_1^+	2.75	2.94	2.82	3.04	2.68	2.79
2_2^+	2.42	2.54	2.49	2.62	2.40	2.41

state multiplet $E(6^+) = 3.24$ MeV. Other approaches to estimating the *np*-pairing energy (e.g., by averaging over the nuclei with isospin $T = 0$ [46]) produce a value that is too high ($\Delta_{np} = 4.08$ MeV). Thus, an estimate of *np*-pairing for odd–odd nuclei in the state with isospin $T = 1$ based on the neighboring even–even nuclei is more realistic:

$$\begin{aligned}\Delta_{np}(N, Z) &= \frac{1}{2}(\Delta_{np}(N-1, Z+1) \\ &+ \Delta_{np}(N+1, Z-1)) \\ &= \frac{1}{2}(\Delta_n(N-1, Z+1) + \Delta_p(N-1, Z+1) \\ &+ \Delta_n(N+1, Z-1) + \Delta_p(N+1, Z-1)),\end{aligned} \tag{31}$$

This relationship agrees with estimate (30).

The ground state multiplet levels with odd $J^P = 1^+$, 3^+, 5^+, 7^+ located below the levels with even J are also clearly visible in the spectrum of excited states of ^{42}Sc.

Thus, a neutron–proton pair above the doubly magic core in an odd–odd ^{42}Sc nucleus forms a ground state multiplet that consists of two groups of levels: the ones with even spin J values and isospin $T = 1$ and levels with odd values of J and $T = 0$. The first group with $T = 1$ consists of levels analogous to the levels of multiplets of neighboring even–even isobaric nuclei ^{42}Ca and ^{42}Ti. The interpretation of the position of levels of the multiplet with $T = 0$ presents considerable interest in the context of analyzing the isospin dependence of pairing forces and requires further study.

CONCLUSIONS

The effect of nucleon pairing in atomic nuclei is a striking manifestation of the quantum-mechanical nature of these nuclei and has extensive theoretical and experimental implications. The present work was aimed at tracing the connection between the structure of spectra of certain atomic nuclei and the effect of nucleon pairing using the simplest models.

Various manifestations of the nucleon pairing effect were mentioned in the introductory section. One of the most striking manifestations of this effect is found in the fact that the ground state of all even–even nuclei is the state $J^P = 0^+$. The short-range attractive forces that act between a pair of nucleons form an energy gap, which corresponds to the energy of breakdown of a pair of nucleons, in the spectra of even–even nuclei.

Nucleon pairing is manifested in the nuclear binding energy and produces the so-called even–odd effect (layering of the mass surface of nuclei with even and odd A). Therefore, the pairing energy may be estimated from the difference in nucleon separation energies for two neighboring nuclei. If the nucleon number is even, additional energy corresponding to the pairing energy is required to break down a pair.

We have compared different methods for determining the even–odd effect magnitude Δ_n and Δ_p based on the experimental binding energy values and certain analytical approximations. The calculation of Δ_n and Δ_p using four experimental binding energy values allows one to compensate for the systematic distortions that arise due to the mass surface curvature. The use of a greater number of experimental binding energy values leads to no significant improvements in the pairing energy calculations and may even lead to an increase in the error of the even–odd effect determination due to the use of insufficiently accurate measurements of binding energies of short-lived radioactive nuclei when moving away from the stability line.

The simplest method for describing the effects of nucleon pairing within the framework of the one-particle shell model consists in introducing the residual interaction in the form of an attractive δ-potential. The degenerate state of two identical nucleons $(n_1, l_1, j_1) = (n_2, l_2, j_2)$ in the presence of the residual interaction is manifested as a multiplet of the ground state of the nucleus. The splitting magnitude may be determined from the experimental binding energies of atomic nuclei: $\Delta_{nn} = 2\Delta_n$ and $\Delta_{pp} = 2\Delta_p$. The comparison of the excitation energy of the last level of the multiplet $E(J_{\max})$ with the even–odd effect magnitude showed that the calculations of EOS based on three experimental binding energy values systematically overestimate its magnitude. The analysis of the spectra of semimagic even–even nuclei showed that pairing

energies Δ_{nn} (Δ_{pp}) retain correspondence to the multiplet splitting, not only in the presence of a single pair above the core, but also as the shell is filled with pairs of identical nucleons. Thus, a unique correspondence exists between the pairing energy calculated based on the experimental binding energy values and the splitting of the ground state multiplet in the experimental spectrum of excited states of the nucleus. This allows one to predict, judging from the pairing energy value, the presence of excited states with a certain J^P in the given region. The presence of a clearly manifested ground state multiplet allows one to determine, judging from the pairing interaction energy measured experimentally, the basic configuration of a pair producing the prevalent contribution to the ground state. Our calculations revealed a systematic overestimation of the energies of states in a multiplet with small J relative to the experimental data. This discrepancy points first and foremost at the necessity of taking the admixtures of other pair configurations in the ground and excited states of nuclei into account. The entire body of data on the chains of even–even isotopes and isotones points at a connection between the pairing interaction and the collective degrees of freedom.

The question of the nature of the first excited state 2^+ in even–even nuclei that lies below the pairing energy is the most interesting one. On the one hand, the first excited state 2^+ should be in the ground state multiplet, but calculations systematically overestimate the value of its energy. On the other hand, the spectra of low-lying levels in nuclei with $Z < 20$ have a marked vibrational nature. The state of even–even nuclei with a pair of nucleons above the doubly magic core is spherically symmetric at $J = 0$. However, since the difference between the pairing energy and the deformation energy is small, collective excitations should be easily triggered in such systems. Therefore, quadrupole oscillations may arise, and level 2_1^+ is a superposition of pairing correlations of nucleons and collective excitations. The analysis of nuclei systematics allows one not only to isolate analog states in the nuclear spectra, but also to reveal analogies in the nucleon–nucleon pairing strength and specify the isospin dependence of the pairing interaction.

The question of the strength of pairing forces that act between a proton and a neutron Δ_{np} presents considerable interest [45–47]. A study of the multiplet of analog states $T = 1$ in an odd–odd nucleus may provide the data on the nucleon pairing strength, and a comparison of states with $T = 1$ and $T = 0$ may clarify the isospin dependence of pairing forces. The results of calculating the ground state multiplet of ^{42}Sc were presented, and it was shown that the pairing of a neutron and a proton in state $T = 1$ is analogous to the pairing of identical nucleons in the neighboring even–even nuclei. The multiplet structure and the magnitude of its splitting suggest that *np*-pairing forces in ^{42}Sc are of the same order of magnitude as the forces that act between a pair of neutrons in ^{42}Ca and a pair of protons in ^{42}Ti: $\Delta_{np}(T = 1) = 3.44$ MeV.

ACKNOWLEDGMENTS

The authors would like to thank N.N. Peskov for technical support of this study.

REFERENCES

1. R. B. Wiringa, V. G. J. Stoks, and R. Schiavilla, Phys. Rev. C: Nucl. Phys. **51**, 38 (1995).
2. C. F. von Weiszzcker, Z. Phys. **96**, 431 (1935).
3. H. A. Bethe and R. F. Bacher, Rev. Mod. Phys. **8**, 165 (1936).
4. M. G. Mayer and J. H. D. Jensen, *Elementary Theory of Nuclear Shell Structure* (New York, 1955).
5. J. Bardeen, L. N. Copper, and J. R. Schrieffer, Phys. Rev. **108**, 1175 (1957).
6. N. N. Bogolyubov, Nuovo Cimento **7**, 794 (1958).
7. S. T. Belyaev, Kgl. Danske Videnskab. Selskab, Mat.-fys. Medd. **31**, no. 11, 1 (1959).
8. V. G. Solov'ev, Zh. Eksper. Teor. Fiz. **35**, 823 (1958).
9. V. G. Soloviev, Nucl. Phys. A. **9**, 655 (1958).
10. V. G. Solov'ev, *Atomic Nuclear Theory: Nuclear Models* (Moscow, 1981) [in Russian].
11. J. M. Eisenberg and W. Greiner, *Nuclear Theory. Vol. 3. Microscopic Theory of the Nucleus* (Amsterdam, 1972).
12. P. Ring and P. Schuck, *The Nuclear Many-Body Problem* 3rd ed., (Berlin, 2004).
13. D. J. Rawe and J. L. Wood, *Fundamentals of Nuclear Models, Foundational Models* (Singapure, 2010).
14. G. Audi, M. Wang, A.H. Wapstra, F.G. Kondev, M. MacCormick, X. Xu, and B. Pfeiffer, Chinese. Phys. C **36**, p. 1287; M. Wang, G. Audi, A. H. Wapstra, F. G. Kondev, M. MacCormick, X. Xu, and B. Pfeiffer, Chinese Phys. C **36**, 1603 (2012).
15. Evaluated Nuclear Structure Data File. Brookhaven, National Nuclear Data Center. http://ie.lbl.gov/ensdf/
16. Data Base. Tsentr Dannykh Fotoyadern. Eksper. Nauchn.-Issl. Inst. Yadern Fiz. Mos. Gos. Univ. http://cdfe.sinp.msu.ru/
17. A. Bohr and B. R. Mottelson, *Nucl. Structure* Vol. 1 (New York, 1969).
18. D. G. Madland and J. R. Nix, Nucl. Phys. A., **476**, 1 (1988).
19. P. Moller and J. R. Nix, Nucl. Phys. A., **536**, 20 (1992).
20. T. Duguet, P. Bonche, P.-H. Heenen, and J. Meyer, Phys. Rev. C: Nucl. Phys. **65**, 014311 (2002).
21. A. S. Jensen, P. G. Hansen, and B. Jonson, Nucl. Phys. A. **431**, 393 (1984).
22. A. E. S. Green and D. F. Edwards, Phys. Rev. **91**, 46 (1953).
23. M. Liu, N. Wang, Y. Deng, and X. Wu, Phys. Rev. C: Nucl. Phys. **84**, 014333 (2011).
24. J. Margueron, H. Sagawa, and K. Hagino, Phys. Rev. C: Nucl. Phys. **77**, 054309 (2008).

25. P. Vogel, B. Jonson, and P. G. Hansen, Phys. Lett. B **139**, 227 (1984).
26. P. Moller, J. R. Nix, W. D. Meyers, and W. J. Suratecki, At. Data Nucl. Data Tables **59**, 185 (1995).
27. G. Royer, M. Guilbaud, and A. Onillon, Nucl. Phys. A **847**, 24 (2010).
28. N. Wang and M. Liu, J. Phys. Conf. Ser. **420**, 012057 (2013).
29. D. Lunney, J. M. Pearson, and C. Thibault, Rev. Mod. Phys. **75**, 1021 (2003).
30. I. Talmi, in *Contemp. Concepts in Phys. Vol. 7. Simple Models of Complex Nuclei* (Harwood Academic, New York, 1993).
31. J. P. Schiffer and W. W. True, Rev. Mod. Phys. **48**, 191 (1976).
32. L. C. Biedenharn and J. D. Louck, *Angular Momentum in Quantum Physics* (Mass. 1981).
33. G. Racah, Phys. Rev. **63**, 367 (1943).
34. M. Bender, P.-H. Heenen, and P. C. Reinhard, Rev. Mod. Phys. **75**, 121 (2003).
35. W. Satula, J. Dobaczewski, and W. Nazarewicz, Phys. Rev. Lett. **81**, 3599 (1998).
36. J. Dobaczewski, P. Magierski, W. Nazarewicz, W. Satuła, and Z. Szymański, Phys. Rev. C: Nucl. Phys. **63**, 024308 (2001).
37. W. A. Friedman and G. F. Bertsch, Eur. Phys. J., A **41**, 109 (2009).
38. I. M. Green and S. A. Moszkowski, Phys. Rev. **139**, 790 (1965).
39. A. Plastino, R. Arvieu, and S. A. Moszkowski, Phys. Rev. **145**, 837 (1966).
40. S. A. Moszkowski, Phys. Rev. C: Nucl. Phys. **2**, 402 (1970).
41. S. A. Moszkowski, Phys. Rev. C: Nucl. Phys. **19**, 2344 (1979).
42. A. Heusler and P. von Brentano, Eur. Phys. J., A **38**, 9 (2008).
43. D. S. Delion, R. J. Liotta, P. Schuck, A. Astier, and M.-G. Porquet, Phys. Rev. C: Nucl. Phys. **85**, 064306 (2012).
44. B. Buck, A. C. Merchant, and S. M. Perez, Phys. Rev. C: Nucl. Phys. **77**, 017301 (2008).
45. D. J. Dean and M. Hjorth-Jensen, Rev. Mod. Phys. **75**, 607 (2003).
46. A. O. Macchiavelli, P. Fallon, R. M. Clark, et al., Phys. Rev. C: Nucl. Phys. **61**, 041303 (2000).
47. P. Sorlin and M.-G. Lorquet, Prog. Part. Nucl. Phys. **61**, 602 (2008).

Translated by D. Safin